International Journal of Automotive Technology, Vol. 17, No. 6, pp. 947–958 (2016)
DOI 10.1007/s12239–016–0092–z

pISSN 1229–9138/ eISSN 1976–3832

THERMOMECHANICAL BEHAVIOR OF THE PISTON OF AN AIR-COOLED DIESEL ENGINE IN SEMI-PERMANENT MODE

T. HEDHLI* and J. BESSROUR

Laboratory of Applied Mechanics and Engineering, University Tunis El Manar,
National School of Engineers of Tunis, BP37, The Belvedere, Tunis 1002, Tunisia

(Received 16 December 2015; Revised 2 March 2016; Accepted 30 March 2016)

ABSTRACT–The pistons of the diesel engines are currently used under increasingly high loadings. Crackings are sometimes observed without understanding their causes. This work is one of the studies contributing to the comprehension of the mechanisms at the origin of these problems and their modeling by the identification of the parameters which would make it possible to interpret the causes of these faulty operations. This study has permitted the development of a three-dimensional numerical simulation model of the coupled thermomechanical and dynamic behavior of an air cooled diesel engine piston. This study has particularly led to a realistic description, in semi-permanent mode, fields of temperatures, stresses and strains according to the mode and engine load and to identify the most solicited zones which constitute the zones at risk. The fatigue analysis of the endurance diagrams showed that the piston functions in the case of extreme loadings.

KEY WORDS : Diesel engine, Air cooling, Piston, Thermomechanical behavior, Dynamic, Numerical simulation, Finite elements, Fatigue

1. INTRODUCTION

The pistons of the engine of a vehicle are currently subjected to increasingly severe cyclic loading. Surface or even in-depth damages are sometimes observed during diagnoses without understanding their causes. Moreover, the real thermomechanical behavior of the internal combustion engines was always difficult to control, as well as the apprehension of the influence of certain operation parameters on their mechanical resistances. The case of direct injection standard diesel engine DEUTZ F8L413, cooled by air, is particularly problematic.

The complexity of the environment where evolves the aluminium to silicon alloy piston, with regulating room, of such engine characterized by an operation under severe thermal conditions (air cooled cylinder and piston cooled by oil jet) and the various interactions fluid and wall of the piston-cylinder unit are the main causes.

Several studies were developed in the field of piston thermals based on very simplified models in the beginning, like two-dimensional rheological models (1960), the simplified analytical (1970). Then numerical models were developed as since the Eighties. The two-dimensional numerical models based on the finite element method continue to be developed until now. Moreover, we finds other more recent studies (Monro *et al*., 1990; Wang *et al*., 1995) which developed respectively 3D numerical and axisymmetric models in order to determine the field of temperature and to carry out a better thermo-tribological performance. However, most quoted work tackle only the thermal problem of the piston separate from the mechanical problem. In addition, the numerical simulations, often in permanent mode, use averaged thermal exchange coefficients realised for each phase of the driving cycle. The interaction with the cylinder was made according to a rough estimate of the cylinder walls temperature.

We propose in this work, a three-dimensional model of analysis in semi-permanent non-stationary mode of the thermo-mechanical and dynamic behavior of a piston. We consider as a study case the air cooled engine DEUTZ F8L413 functioning under very severe thermal conditions. The adopted numerical model, based on the finite element method, has the advantage of using, as boundary conditions, the values of certain parameters taken on an experimental test bed reproducing the engine operation real conditions. We are particularly interested in the modes of maximum torque and maximum power. The dynamic loadings (efforts and accelerations) will be calculated instantaneously throughout the operation cycle, attributing to the problem the nonstationary character over one period. This dynamic study is based on a shifted axis piston kinematics. The thermal problem will be initially treated in permanent mode starting from the coefficients of exchange, gas side, averaged over a period and will be followed by a calculation in variable mode with instantaneous exchange coefficients along a cycle. The results will particularly enable us to identify the distribution of the heat fluxes around the piston.

**Corresponding author.* e-mail: Taher.Hedhli@enit.rnu.tn

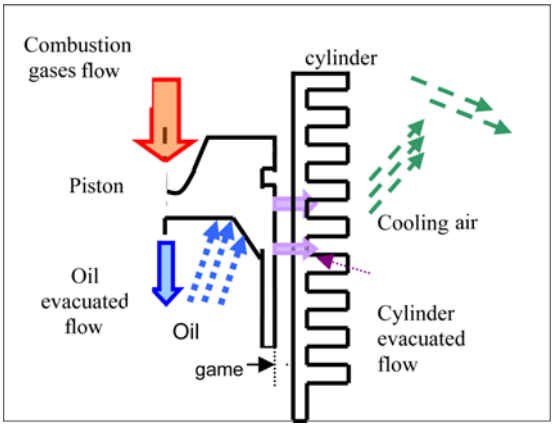

Figure 1. Thermal flux through the piston walls (Cooling by air, and oil).

The description of the fields of stresses of thermo-mechanical origins in the structure has allowed us to identify the most solicited areas which constitute the zones at risk in surfaces and in depths. To validate the dynamic endurance, it offers an analysis of the behavior in fatigue, around these areas, using the criterion of Haigh. The identification of zones at risk for this type of engines operating in extreme conditions makes it possible to support research on the optimization and improvement of the design of its bodies.

2. PISTON THERMAL PROBLEM

The thermal flux, originated from the combustion gasses, occurs mainly in the head of the piston by convection (Hedhli and Mejri, 2007). After the transitional stage, during which the piston accumulates a quantity of heat which increases its temperature, this heat flow will be evacuated, in a permanent regime, partially by the piston side surface toward the air cooled cylinder, and by the oil jets on the internal face.

The piston of such an engine, is thus, submitted to an intense thermal and mechanical loading;

- Excessive thermal expansion of the piston can lead to a degradation of the slack with the cylinder and drastically affect the friction, oil consumption, engine noise and the unit lifetime.
- The necessity for maintaining the temperature of an aluminum alloy piston below a certain maximum value, led to the need to study the heat fluxes which cross it.
- In addition, this leads us to visualize the fluctuations of the maximum equivalent stress (Von Mises) compared to the elastic limit of the material and check if the piston has a good mechanical strength in fatigue.

3. EXPERIMENTAL STUDY

The objective of the experimental study, is initially to permit the determination of the characteristic curves of the engine (torque, power and specific consumption), to set an overall energy assessment and measure certain operation parameters, which will be injected as boundary conditions in the numerical model. Note that one of the objectives of the numerical analysis is to allow the determination of some internal parameters not accessible to measurements (temperatures, strains and stresses).

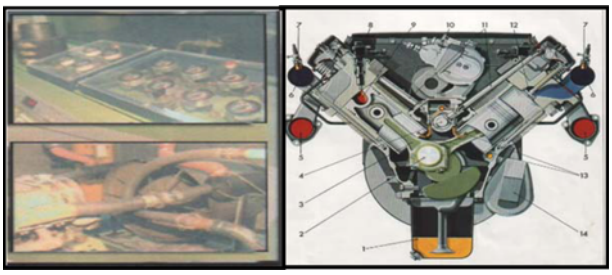

Figure 2. Test bench and engine diagram (8 cylinders in V).

It will have the advantage of placing the engine loaded with a hydraulic brake system under conditions similar to a loading on a vehicle.

The engine is loaded by a hydraulic brake (Figure 2), the whole unit being remotely driven. The test bench is equipped with an air cooling blower and sensors to take the various parameters (torque, speed, temperatures, pressures, air flow, fuel flow, etc.).

This experimental procedure has allowed us to;

- Draw the characteristic curves of the engine at full load (Figures 3 ~ 5) and to identify the modes of maximum power (2,650 rpm), maximum. torque (1,400 rpm) and minimum consumption (1,600 rpm) (Table 2).

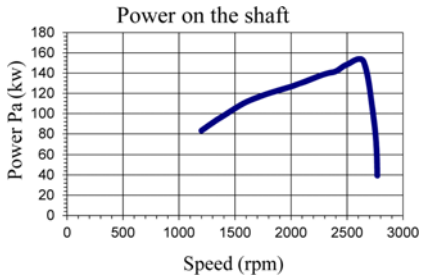

Figure 3. Power on the shaft.

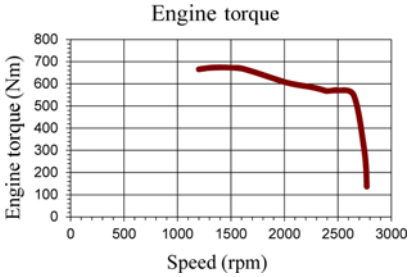

Figure 4. Engine torque.

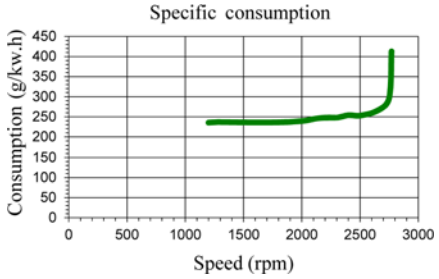

Figure 5. Specific consumption.

Table 1. Measured temperatures.

N (rpm)	Temperature of the cylinder wall (C)			Oil temperature (C)
	TDC	Middle	BDC	
2,650	150	125	125	99.8
1,600	135	120	120	92
1,400	135	120	120	90.3

Table 2. Measured performances.

N (rpm)	P (kw)	Cm (Nm)	Cs (g/kw h)	P_{air} (KW)	P_f (KW)	Excess air
2,650	150	547	265	94	117	1.1
1,600	111	669	236.1	89	91	1.6
1,400	98	674	236.4	83	79	1.6

These modes were selected thereafter for numerical simulations of the study,

- Measure, for each point of operation, the air cooling power P_{air},
- Measure the actual flow rate of air intake, the fuel flow and deduct the excess air,
- Measure the temperature of the exhaust gas and infer the power of smoke P_f (Table 1),
- Measure, using a proper disposition, the temperature of the cylinder at TDC (top dead center), middle and BDC (bottom dead center), as well as the temperature of the oil (Table 1), since these values are, subsequently, input into the numerical model (boundary conditions of the thermal problem).

The measurement of the cylinder wall temperatures carried out at selected points (TDC, middle and BDC), for the considered engine modes will allow the assessment of the wall temperature $T_{w\text{-}int}(z)$ inside the cylinder according to height z. To this effect, we proceeded to an extrapolation along the z-axis by using the analytic expression proposed by Wang *et al*. (1995) describing the evolution of the interior temperature along the piston travel in function of temperatures Tph et Tpb of the TDC and BDC;

$$T_{w-int}(z) = T_{ph} - (T_{ph} - T_{pb})^{e^{\frac{-50}{1,45z}}} \quad (1)$$

These temperatures will be input thereafter in the numerical model as boundary conditions for the convection model of the piston side.

4. THERMODYNAMIC CYCLE

The objective of the indicated cycle plot is initially to be able to use it in the piston-gas instantaneous convection exchange coefficient calculation model hg, which depends on the pressure P_g and the temperature T_g of gases at each piston position.

Besides, it will be also used to determine, for the selected modes, the specified work (equal to the area of the cycle) and to deduce the mechanical efficiency and the mechanical losses by comparison with the measured values of the mechanical work on the shaft.

The model chosen for this purpose is the cycle of Sabathe (partially combustion at constant volume and at constant pressure). The plot of the indicated cycle (Figures 6 and 7) is performed on the basis of geometrical data (rolled, travel and compression rate), angles of distribution (advance and delay to the opening and closing of the intake and exhaust, injection advance), some parameters measured on the bench including the consumed fuel mass per cycle,

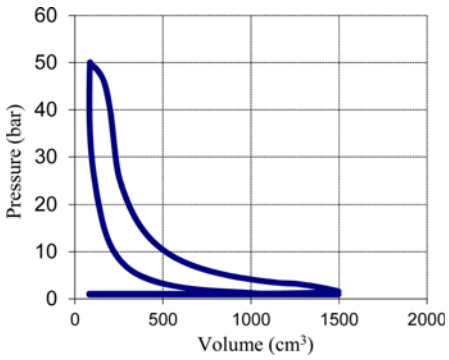

Figure 6. Indicated cycle at max power (2,650 rpm).

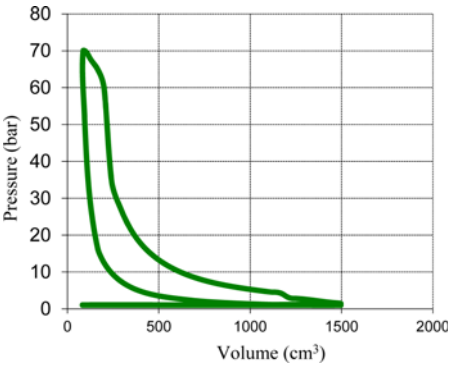

Figure 7. Indicated cycle at max torque (1,400 rpm).

Table 3. Performances from indicated cycles.

Engine speed (rpm)	Organic efficiency	Average pressure indicated (bar)	Mechanical losses (KW)
2,650	0.851	7	22.5
1,400	0.824	9	14.6

and some reasonable assumptions.

The area of the cycle, calculated by the trapezoids method, corresponding to the indicated work by cycle, makes it possible to calculate the organic output starting from work on the shaft measured on the test bench and to deduce the mechanical losses from them. It also allows the calculation of the indicated average pressure of the cycle (Table 3).

5. PISTON THERMAL ANALYSIS

The thermal problem clarification allows the study of the temperature distribution in an established mode. The stationary mode is obtained by the resolution of the equation of heat in non-linear permanent mode (the conductivity coefficient K is a function of temperature) without heat source (Reipert *et al.*, 1984);

$$\frac{\partial}{\partial x}\left(K(T)\frac{\partial T}{\partial x}\right)+\frac{\partial}{\partial y}\left(K(T)\frac{\partial T}{\partial y}\right)+\frac{\partial}{\partial z}\left(K(T)\frac{\partial T}{\partial z}\right)=0 \qquad (2)$$

The boundary conditions on the border surfaces are, for the majority, the convection conditions which are expressed using the condition of Neuman:

$$\vec{n}(K\overrightarrow{\nabla T})+h(T-T_{\infty})=0 \qquad (3)$$

where h is the thermal convection coefficient. The determination of this coefficient is relatively complex as a result of the gases temperature variation and the surface exchange due to the piston movement.

5.1. Combustion Chamber Thermal Transfers

For a given mode, the variation of temperature T_g, pressure P_g, and gases speed in the chamber as a function of the crankshaft rotation angle, imply the cyclic variation of the convection coefficient h_g in the chamber. The problem is to seek an expression of the coefficient h_g within the context of thermal transfers in the engines. Several models were proposed with the advantage of describing the influence of the standard parameters for the engines like T_g, P_g and the average velocity of the piston V_m (Techniques de l'ingénieur BM 2900, 2004).

EICHELBERG Correlation: $h_g = 0{,}78 \,.\, \sqrt[3]{V_{moy}}\,\sqrt{P_g \,.\, T_g}$ (4)

BRILLING Correlation: $h_g = 0{,}99.(3{,}5+0{,}185.V_m)\sqrt[3]{P_g.T_g}$ (5)

WOSCHNI Relationship: $h_g = 0.013.D^{-0.2}P_g^{0.8}.T_g^{-0{,}53}.V^{0{,}8}$ (6)

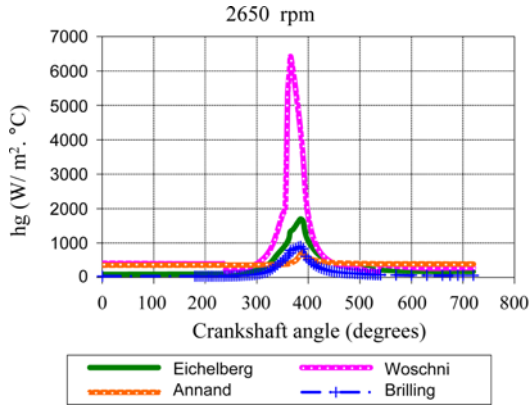

Figure 8. hg at maximum power mode (2,650 rpm).

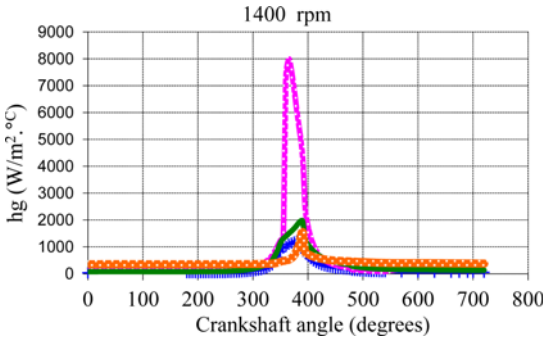

Figure 9. hg at maximum torque mode (1,400 rpm).

Such that D is the diameter of the piston and V is a characteristic velocity dependent on the piston average speed of the unitary displacement and the two specific coefficients to each cycle phase.

ANNAND Relationship: $h_g = a.\frac{K_g}{D}.\mathrm{Re}^{0.7}+c$ (7)

Re is the Reynolds number of the gases in the cylinder. Figures 8 and 9 represent the instantaneous h_g value according to the crankshaft angle during a complete cycle;

Currently it is the relationship of Woschni which is used universally by all authors for good conformity with experimental results.

Because the cyclic variation of the thermal exchange coefficient h_g, a semi-steady mode was considered by adopting an average value over a cycle $\overline{h_g}$ combined with an average temperature of the gases weighted by the coefficient h_g;

$$\overline{T_g}=\frac{1}{\overline{h_g}}\int\frac{h_{gi}T_{gi}}{4\pi}d\alpha=\frac{1}{\overline{h_g}}\left[\overline{h_gT_g}\right] \qquad (8)$$

5.2. Oil Convection

The system used by manufacturers to cool the piston from behind is a spray from a pressurized oil jet. Exchanges are

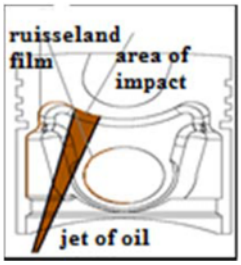

Figure 10. Piston Cooling by jet of oil.

then purely convective between the bottom walls of the piston and the oil.

The adopted convection coefficient is calculated by the following equation using the density ρ_h and the oil viscosity μ_h (Techniques de l'ingénieur B2800, 1996);

$$h_h = 68,2\sqrt{R_m.N.\frac{\rho_h D_i}{\mu_h}} \quad (9)$$

R_m is the radius of the crankpin, D_i is the nozzle diameter and N the rotation speed.

5.3. Transfer Condition between Piston and Cylinder

To characterize the thermal exchange between the sidewall of the z-axis piston and the cylinder through the oil film interposed in the clearance, we adopted the equivalent overall convective model proposed by Wang *et al*. (1995) for r = Re (piston outer radius);

$$-K\frac{\partial T}{\partial r} = \beta(z)(T - T_w(z)) \quad (10)$$

Such that T_w is the temperature of the cylinder wall measured on the test bench and the β(z) value is estimated according to the axial position (crown, ring zone and piston skirt) (Wang *et al*., 1995).

6. UNBALANCED PISTON DYNAMIC PROBLEM

It is about a piston with an incorporated combustion pre-chamber (regulating chamber) in aluminum alloy of 120 mm diameter. Figure 11 is a graphical representation of the piston:

6.1. Kinematic Characterization

The piston moves in the cylinder at an off-axis relative to the axis of the latter to the value C_p and passing through its center of gravity (Tahar Abbes *et al.*, 2001). The acceleration of the piston, moving axially within the cylinder, is determined from the mechanism Connecting rod-crank given by the following figure;

The instantaneous position of the piston is given by

s = OB-O'A'. Or O'A' = O'H + HA', O'H = OK = r cosθ and HA' = $(A'M^2 - HM^2)^{0.5}$ with A'M = l and HM = HK + KM = Cp + r sinθ.

Figure 11. Geometric model of the piston.

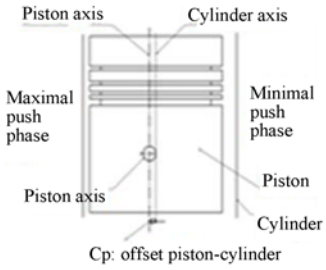

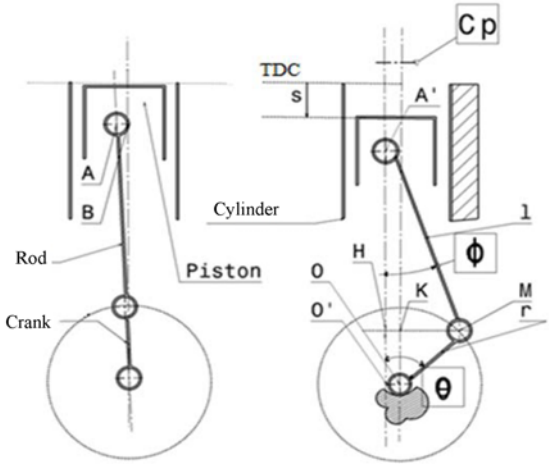

Figure 12. Position of the piston at TDC.

OA = r + l, AB = C_p and
OB = $(OA^2 - AB^2)^{0.5} = [(r + l)^2 - C_p^2)]^{0.5}$.

Knowing that: HM = HK + KM = C_p + r sinθ and A'M = l, then;

$$S = [(1+r)^2 - C_p^2]^{0.5} - \{r\cos\theta + [l^2 - (C_p + r\sin\theta)^2]\}^{0.5}$$

if C_p + r sinθ = B, the position of the piston is written;

$$S = ((1+r)^2 - C_p^2)^{0.5} - (r\cos\theta + (l^2 - B^2)^{0.5}) \quad (11)$$

The axial speed is

$$V = \frac{dS}{dt} = r\frac{d\theta}{dt}\sin\theta + Br\frac{d\theta}{dt}(l^2 - B^2)^{-0.5}\cos\theta .$$

With $\frac{d\theta}{dt} = \omega$ crankshaft rotational speed

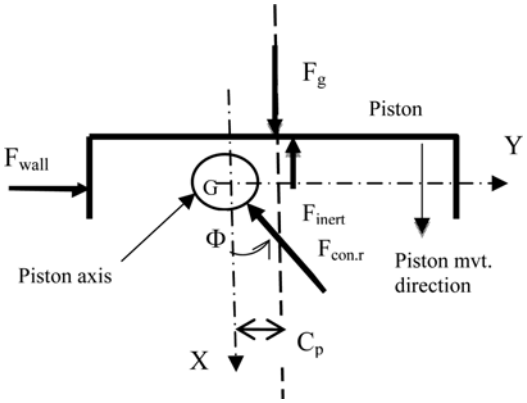

Figure 13. Efforts on the piston.

$$V = r\omega\sin\theta + \frac{Br\omega\cos\theta}{(l^2 - B^2)^{0.5}} \quad (12)$$

The axial acceleration is

$$\gamma = r\omega^2\cos\theta + \frac{(Br\omega\cos\theta)^2}{(l^2 - B^2)^{\frac{3}{2}}} + \frac{(r\omega\cos\theta)^2 - Br\omega^2\sin\theta}{(l^2 - B^2)^{\frac{3}{2}}} \quad (13)$$

6.2. Dynamic Characterization

The axis of the piston is always to the left of the cylinder axis, as seen in front view of an engine piston rotating clockwise (Figure 13).

The maximum thrust side of the piston is in the perpendicular to the piston axis. This is the side which supports the greatest thrust force, represented by the lateral force, which pushes the piston against the cylinder wall. The maximum thrust side is the left side.

The axis giving the stroke of the piston, positively oriented toward the bottom, has its origin coincides with the piston TDC. The piston position s, the axial speed V and the acceleration γ along the cylinder are given according to the crankshaft angle θ. The piston, in his movement, always follows a straight direction parallel to the cylinder axis called the piston axis. These two axes are offset with respect to each other of the C_p value and it is the piston axis containing its center of gravity which undergoes this offset. The piston, isolated, is instantly in balance under the effect of the following forces (Arques, 1987);

F_g : Force of gases,
F_c : Force of the connecting rod connection,
F_i : Inertia force of the piston and its axis,
F_w : Lateral force of the cylinder wall on the piston.

If G is the center of gravity of the piston-axis assembly, and ϕ and the pivot angle of the connecting rod around G, we write the equilibrium equations in the coordinate (G, x, y), the friction efforts are neglected;

$$\sum F_X = F_g - F_c\cos\phi - F_i = 0 \quad (14)$$

$$\sum F_Y = F_w - F_c\sin\phi = 0 \quad (15)$$

with $tg\,\phi = \frac{B}{\sqrt{l^2 - B^2}}$ and $B = r\sin\theta + C_p$.

The elimination of F_c of Equations (14) and (15) gives the following equation:

$$F_w = (F_g - F_i)\,tg\phi \quad (16)$$

For a constant crankshaft rotation speed ω, the inertial force of the piston-axis system is $F_i = m\gamma$ where m is the system mass and the acceleration γ is given by the kinematic study as a function of the angle of rotation θ.

Knowing that the gas force is known, and is given by $F_g = P_g A$, where A is the area of the piston head and P_g is the gas pressure (known for each position of the specified cycle), F_w can be easily determined from the Equation (16). The experimental study and the measures taken on the engine Deutz F8L413 give in particular ω = 146,608 rd/s for the regime of maximum torque, the radius of the crank arm r = 0,065 m and the rod length l = 0.2375 m. The offset of the piston is C_p = 0.002 m, the piston mass is m_p = 2,215 kg and that of the axis is m_a = 0,935 kg.

Figure 14 represents the acceleration of the offset piston in function of the rotation angle for two revolutions of the shaft (0° ~ 720°) and Figure 15 gives the forces in Newton. The forces on the isolated piston vary between – 2 and + 8

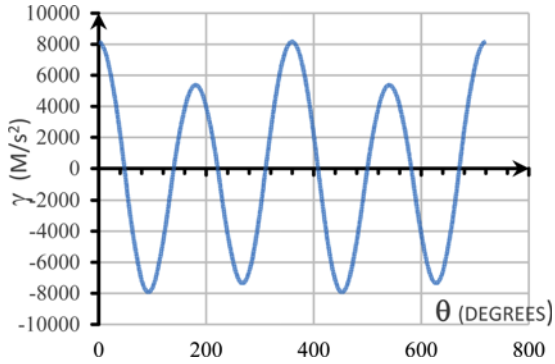

Figure 14. Piston acceleration.

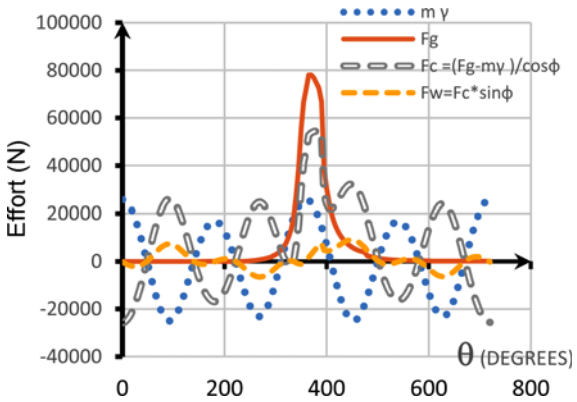

Figure 15. Efforts on the piston.

tons, acceptable values for an engine with combustion pressures ranging from 60 to 80 bars.

7. THERMOMECHANICAL COUPLING AND DYNAMIC LOADING

The coupling of equations thermal and mechanical often makes their resolution difficult (absence of analytical solutions, problems of convergence in the calculation codes and too long calculation times). Therefore, we often seek to simplify these equations by minimizing their coupling. The influence of the thermal on the mechanics is given through the law of conduct which depends on the temperature. To solve the mechanical problem we need to know the temporal evolution of the temperature field. Conversely, we have an influence, in the opposite direction, of the mechanics on the thermal via a source of heat from the structure deformation. This source is negligible compared to the combustion heat.

We have adopted a sequential coupling starting with solving the heat Equation (2) that identifies the range of temperatures τ. This is injected into the thermo-elastic problem, treated with a law of linear behavior, homogeneous and isotropic using the thermal expansion coefficient a and the temperature variation τ. The stress tensor is given by Equation (17) using the coefficients of Lamé λ and μ:

$$\underline{\underline{\sigma}} = 2\ \mu\ \underline{\underline{\varepsilon}} + \lambda\ Tr(\underline{\underline{\varepsilon}}).\underline{\underline{\delta}} - (3\lambda + 2\mu)\ \alpha\ \tau\ .\ \underline{\underline{\delta}} \qquad (17)$$

The strain tensor $\underline{\underline{\varepsilon}}$ is given by (18) using the coefficient of Poisson ν and the module of elasticity E:

$$\underline{\underline{\varepsilon}} = \frac{1+\nu}{E}\ \underline{\underline{\sigma}} - \frac{\nu}{E}\ Tr\ (\underline{\underline{\sigma}})\ \underline{\underline{\delta}} + \alpha\ \tau\ .\ \underline{\underline{\delta}} \qquad (18)$$

7.1. Numerical Simulations

The method adopted is that of finite elements, through the code ABAQUS. Taking into account of the symmetry plane, Figure 16 represents the mesh of a half piston (11500 elements and 20700 nodes).

The discretization is based on Galerkin's method. The elements are quadratics and tetrahedrals (C3D10MT).

The physical, thermal and mechanical characteristics of the aluminum-silicon alloy piston (A-S12UNG) are introduced according to the temperature (Jault, 2001; Laurent and Vuillermoz, 1993; Li, 1986).

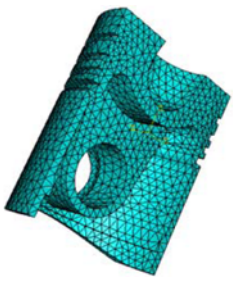

Figure 16. Mesh of piston.

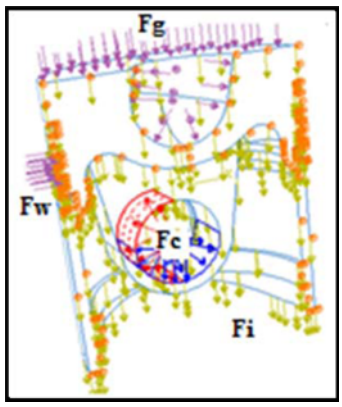

Figure 17. Dynamic loading applied to plunger.

The resolution of the heat equation uses the condition of Neuman (3) with the boundary conditions mentioned above and summarized in these points:

- Convection gas side with the relationship of Woschni (6),
- Convection oil side with the relationship (9),
- Convection cylinder side with the relationship of Wang (10),
- The symmetry plane: zero heat flow.

This resolution leads to the determination of the fields of temperature and thermo-mechanical stresses.

In a next step, dynamic loading is applied to understand the superposition of simultaneous effects caused by thermal and dynamic loading.

The modeling of the instantaneous dynamic loading is to introduce at any moment of the cycle, the inertial forces F_i as forces of volume and the efforts of gas F_g as pressure forces (Figures 6 and 7). The efforts of the rod F_c and cylinder F_w are modeled by representative contact forces on a number of nodes, for which it is necessary to make certain distribution assumptions (Figure 17). Indeed, the cylinder-piston contact areas and piston-axis vary according to the direction and way of these efforts.

The piston is in balance under the effect of these forces determined in 6.2. (Figure 15). The only boundary condition introduced is: the normal displacement to the symmetry plane is assumed to be zero.

The method adopted to solve the dynamic problem is the linear incremental method with an implicit scheme. The increment varies depending on the cycle duration and hence the rotation speed.

8. NUMERICAL RESULTS

Figure 18 shows the temperature field, in permanent regime. The maximum value at the piston is 349 °C at 1,400 rpm (maximum torque) and 263 °C at 2,650 rpm (maximum power). Figure 19 shows the evolution of temperatures along the sidewall of the piston.

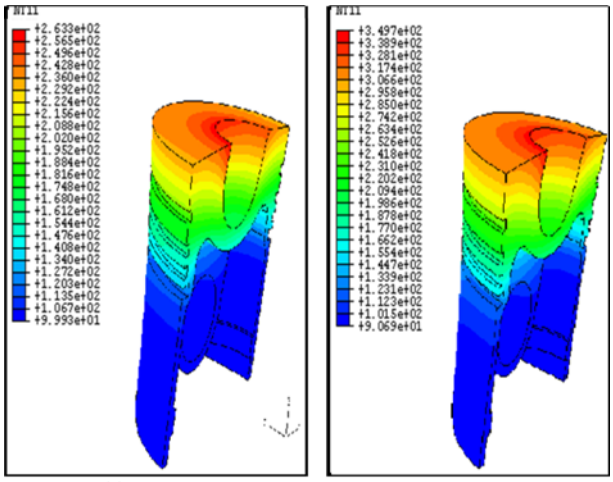

(a) 2,650 rpm (b) 1,400 rpm

Figure 18. Temperature field.

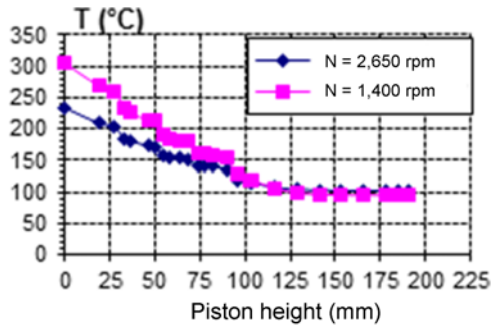

Figure 19. Evolution of the cylinder temperature.

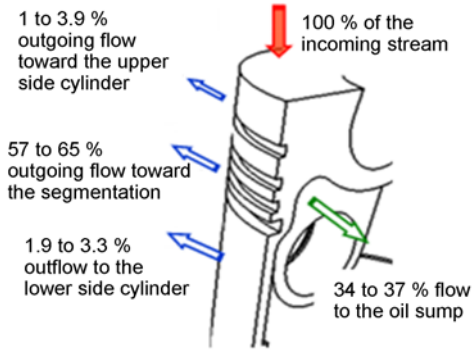

Figure 20. Balance Sheet of the piston thermal flows.

We proceeded thereafter, from the calculated temperatures, to the determination of the piston thermal balance by calculating, by integration, the convective flow on the outer contour. Figure 20 shows the proportions of the flow discharged by the piston towards the oil sump and to the cylinder. It is found that the largest proportion of the stream entering the piston (approximately 60 % to 70 %) is discharged through the air-cooled cylinder.

Figure 21 shows that the piston head is undergoing the

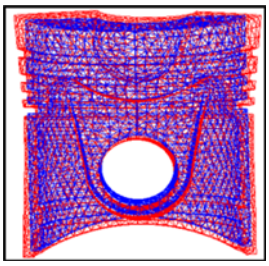

Figure 21. Deflection of the piston.

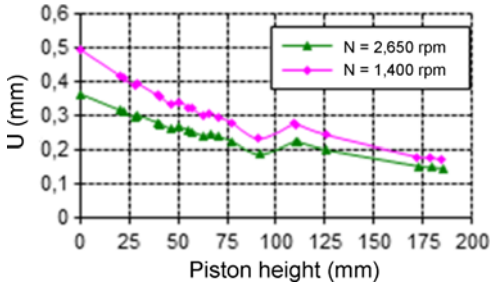

Figure 22. Radial displacement in the normal direction to the axis of symmetry of the piston.

largest expansion and that the travel is elliptical because it is larger in the direction of greater radius of the skirt than in the transverse direction. The radial displacement U (Figure 22) allows the assessment of the minimum clearance between piston and cylinder due to the thermal expansion.

The highest displacement are at the head of the piston, and the latter gets the cylindrical shape as it had the form of a conical skirt at the beginning (hence the name conical skirt piston.).

The highest stress are located at the places that have the highest temperature gradients as the combustion chamber as well as in the areas of lower thickness. These areas are the combustion chamber cavity, the groove of the scraper ring and the inside of the piston (bosses of the skirt at the level of the pin hole to the top). Figure 23 shows the evolution of the total stresses field (thermal and dynamic), at maximum torque, for certain angles of rotation with arrows indicating the areas most solicited.

The evolution of the equivalent stress during a period of time permits to distinguish the disproportion, in each point, of the thermal stress (average stress) and of the stress caused by the dynamic efforts (alternating stress). Figure 24 shows the cyclic changes of the equivalent stress during a cycle at the scraper ring. It is noted that the thermal stress (average stress) is important and note that the overheating is generated by the cylinder force on the piston during the return phase. At the axle hole, we find that the thermal stress is rather low, the temperature at this level is relatively low (90 °C) while the alternating stress due to the connecting rod reactions increases significantly during the combustion-return phase corresponding to the piston descent.

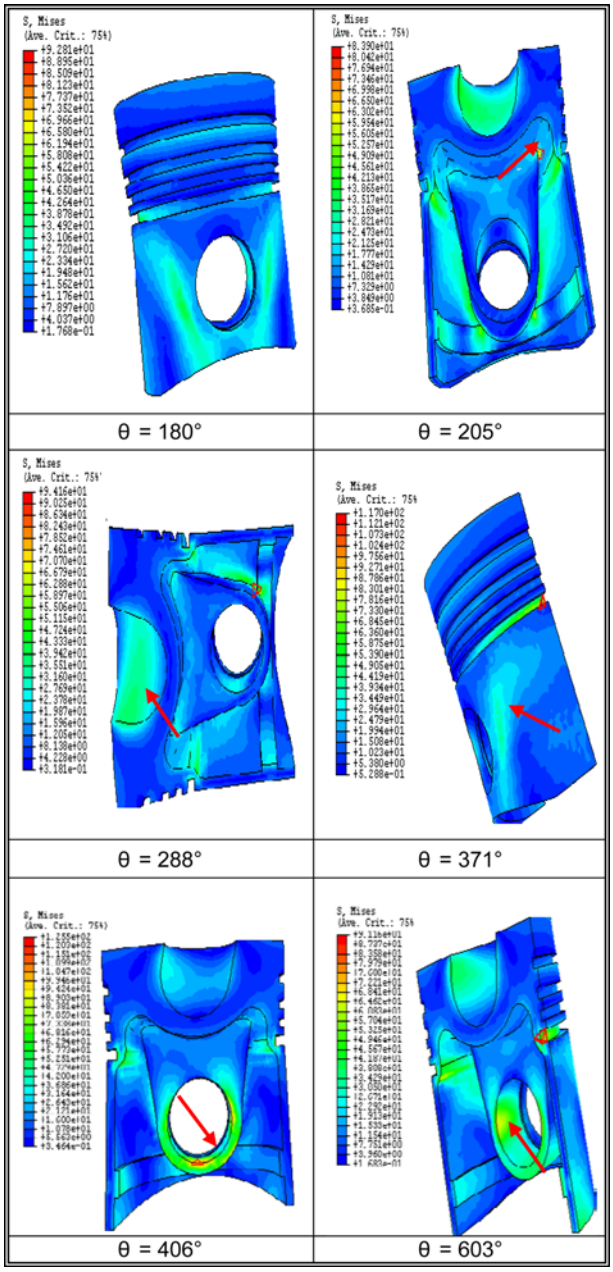

Figure 23. Evolution of the field of Von Mises stress for a few moments of the cycle (Maximum torque).

9. STUDY DURING FATIGUE

The piston, in the course of its operation, is subjected to variable strains over time. These strains lead to cyclic variations in stresses. The breach may occur at the end of a number of cycles N, for a strain amplitude lower than the static breach strain of the material. An analysis during fatigue is necessary to avoid a premature damage (cracking or fracture) likely to lead to more or less short-term damage to the work piece.

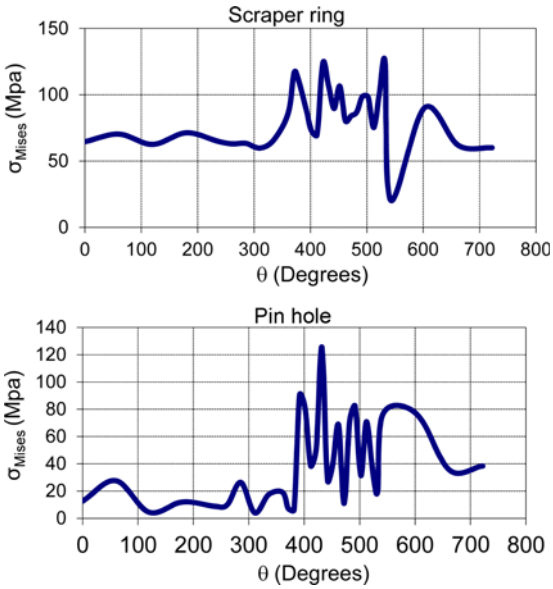

Figure 24. Evolution of the equivalent stress on a cycle (engine speed at maximum torque).

Table 4. Mechanical characteristics.

Material	AS 12 UNG	
Temperature	20 °C to 100 °C	350 °C
R_m (MPa)	215	45
σ_e (MPa)	175	35
σ_D at 10^7 cycles (MPa)	70	30

The adopted endurance diagrams, from the Wohler curves, are plotted as a function of the yield stress σ_E, the tensile strength R_m and the endurance limit at 10^7 cycles σ_D of the measured material based on the temperature. If the temperature increases, σ_E et R_m decrease significantly. Table 4 gives these characteristics for some temperatures;

After the thermal simulation, a diagram is associated to every point according to its temperature. For the study in fatigue and to define a safety factor coefficient, we plotted and used Haigh diagram. This diagram represents the alternating stress amplitude σ_a based on the average stress σ_m and represents the endurance limits. To check the resistance in fatigue with a degree of security, the point which represents a case of loading in service must be located inside the area limited by the two axes and two converging lines. From the stress cyclic evolution in each node at the engine rotational frequency, the average stress σ_m is calculated. The alternating stress σ_a is determined by a Fourier series development to first order. The integrals are calculated by a graphic method (Keita *et al.*, 2014);

$$\sigma_{eq}(x, y, z, t) = \lfloor (\sigma_{eq})_m + (\sigma_{eq})_a \sin(\omega t + \varphi) \rfloor \quad (19)$$

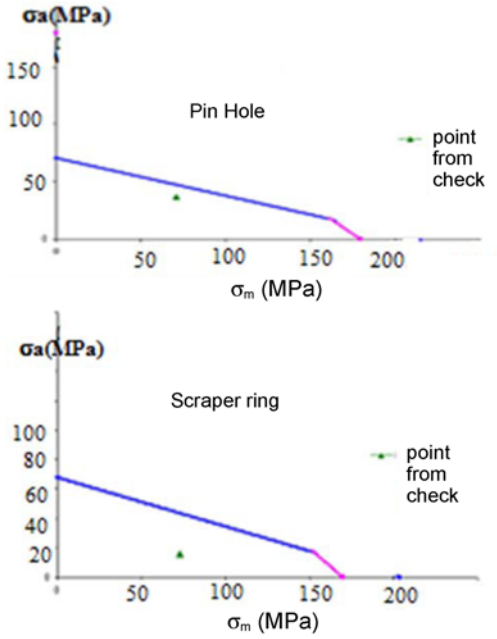

Figure 25. Diagram of haigh.

$$(\sigma_{eq})_m = \frac{1}{T}\int_0^T \sigma_{eq}(x,y,z,t)dt \tag{20}$$

$$(\sigma_{eq})_a = \frac{2}{T}\left\{\left(\int_0^T \sigma_{eq}(x,y,z,t)\cos\omega t dt\right)^2 + \left(\int_0^T \sigma_{eq}(x,y,z,t)\sin\omega t dt\right)^2\right\}^{\frac{1}{2}} \tag{21}$$

Our research of the safety coefficient has involved a number of points where the equivalent stress is maximum at some point of the cycle. Figure 25 shows examples of carried out checks. The observation of Haigh diagrams for the two modes reveals that for maximum torque regime, several points are at the limit of the safe operating area. This effect is due to the importance of the reached operating temperatures as well as the pressure load that is higher than for the other modes. It is found that the areas at risk are the piston head, the pin hole and the pre-combustion chamber.

10. THERMAL FATIGUE IN THE PISTON UPPER SURFACE

The presented thermo-mechanical study has been carried out in permanent regime whereas an average gas convection coefficient and an average gas temperature over a cycle are taken into account. In order to narrow the results by inserting the loading nearest to reality, we have followed the thermal calculation in permanent regime by a calculation in variable mode, at the speed of peak torque, taking the instantaneous gas exchange coefficients and the instantaneous gas temperatures. The calculation has been performed on a few cycles to reach the semi-permanent regime. Thus, we have been able to check that the cyclical temperature fluctuations and stresses remain localized in the upper surface of the piston. These fluctuations are decreasing rapidly in sub-layers and are cancelled out to approximately 2 mm in depth where we find the permanent regime temperatures and stresses (Figure 26). The highest temperature fluctuations at the engine rotational frequency, localized at the surface near the cavity reach 100 °C at maximum torque mode. They cause an alternating stress of ± 60 MPa around an average thermal stress of about 140 MPa (Figure 27). This performance is indicative of a very significant but localized thermal fatigue which may damage the upper piston skin (Szmytka *et al*., 2015).

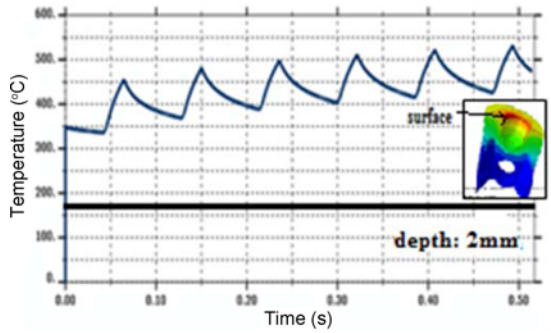

Figure 26. Temperature in semi-permanent mode at maximum torque.

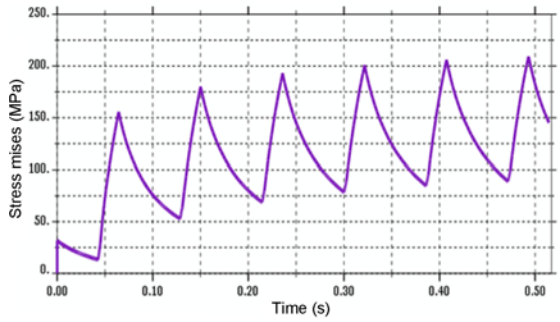

Figure 27. Thermal stresses in semi-permanent mode in upper surface of the piston.

11. SIMULATION RESULTS AND PRACTICAL OBSERVATIONS

The numerical simulations, based on actual loading conditions measured on test bench (regime, maximum torque, temperatures of the cylinder, oil and the intake air), allow to predict, in a realistic manner, the values of non-measurable parameters such as the piston-cylinder hot clearance. They also permit to interpret the causes of

certain damages occurred in practice in some engines.

11.1. Hot Working Clearance Piston-cylinder

The control of this parameter is essential for the mechanical holding, the life expectancy and the efficiency of the engine. The Figure 22 shows that the maximum displacement appears at the head of the piston. But, the diameter of the piston head (119.35 mm) is smaller than the diameter of the skirt (119.89 mm) where the clearance piston-cylinder will be minimal. This cold clearance, given by the manufacturer, is between J_{mini} 0.103 mm and J_{maxi} 0.152 mm. The Figure 22 gives the radial displacement of the skirt (0.18 mm) in 1,400 rpm. Knowing that the minimal radial displacement of the cylinder (Hedhli and Mejri, 2007) is equal to 0.08 mm, it can be deduced that the hot clearance will decrease by 0.1 mm (J_{mini} 0.003 mm and J_{maxi} 0.052 mm).

This hot clearance, determined from the simulations in extreme conditions, is realistic and conducive to a proper functioning of the engine with regard to its allocated technical performances.

11.2. Damages

The numerical simulations showed that this engine, cooled by air, with piston cooled by oil jet, can work in conditions of extreme loads with relatively low safety factors. Certain zones of the piston can undergo a damage by thermal and mechanical fatigue (bottom of the pre-combustion chamber, zones separating the head and the skirt as well as the arbor hole) (Silva, 2006).

The numerical simulations results confirm the damages noticed on certain engines. The signs of overheating and the thermal solicitations localized at the piston head and in the cavity are visible on Figure 28.

The thermal fatigue on the upper surface leads to the

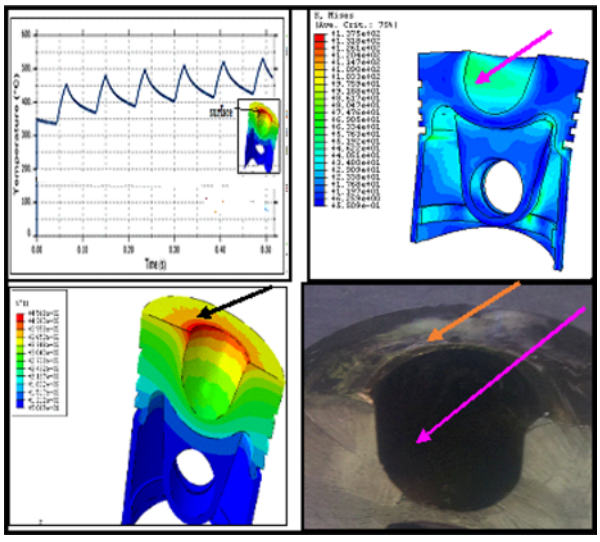

Figure 28. Piston head and cavity: Signs of overheating and thermal stress.

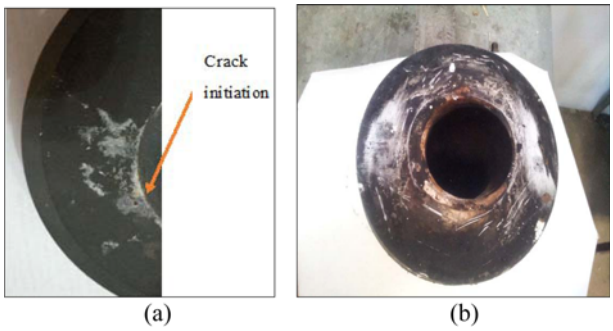

Figure 29. (a) Piston head damages: puncture and crack initiation; (b) Punctures in upper surfaces around the cavity.

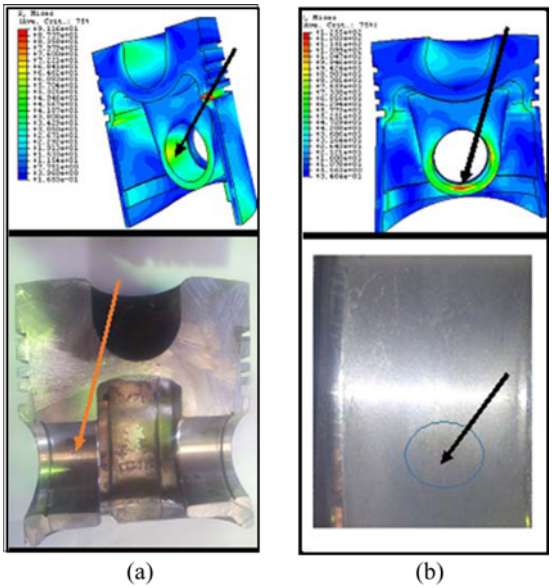

Figure 30. Arbor hole: (a) Damage due to the contact forces with the axis; (b) Scorching.

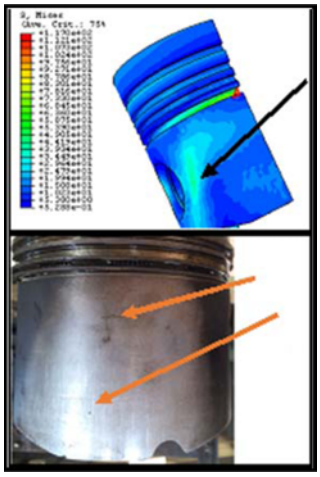

Figure 31. Skirt: Contact surface with the cylinder: Scratches and damage.

appearance of an initiation of cracks and punctures around the cavity (Figure 29). The part of dark color located between the piston head and the pre-combustion chamber (Figure 29) corresponds well to the zone most solicited thermally given by the simulations.

The effect of the high stresses in the arbor hole appears in certain cases as scratches and scorching (Figure 30) due to the high contact forces and friction with the axis. The skirt, where the clearance is minimal, may also suffer wear due to the forces of contact with the cylinder inner wall. Figure 31 shows the damage of a skirt on its most solicited face.

12. CONCLUSION

The damages and the practical observations noticed on several engines having worked in severe conditions confirm the results of the numerical simulations. The air cooled engine, of 120 mm boring, works in limiting conditions.

The pistons of internal combustion engines are among the parts the most solicited and the more complex to model. We still observe the appearance of cracks in the very overloaded pistons of the last generation. The piston can be regarded as the most important element within an engine. The numerical simulation has become a necessary step given the important computational tools development and the considerable reduction of time and development costs.

This work has helped develop a comprehensive three-dimensional model of a thermo-mechanical numerical simulation of an air-cooled diesel engine piston. The advantage of this model is to achieve refined numerical results particularly by the simultaneous consideration of thermal and dynamic loads. Its advantage is to rely on experimental measurements particularly at the piston-cylinder interface.

Thus, the thermal analysis has enabled an identification and a better understanding of the internal mechanisms of the heat flow through the piston and to apprehend the operating regimes that can lead to an overload or to the engine thermal fatigue.

The thermal deformation of the piston allows the prediction of running clearance with the cylinder.

This study has allowed, in particular, to achieve a realistic description, in semi-permanent mode, temperature fields, stress and strain based on the engine mode and load, and to identify the most solicited areas that constitute the areas at risk.

The analysis in fatigue from the diagrams of endurance has shown that certain areas of the piston are functioning in the case of extreme loads. The top surface of the piston can also be the seat of localized thermal fatigue.

This study has allowed us to apprehend and understand the thermo-mechanical mechanisms involved in the complex operation of this piston and to identify the parameters which would allow the interpretation of the anomalies causes (overheating, cracking etc.) appearing during its operation. The influence of extreme weather conditions on engine performance could be simulated by the same methodology.

This modeling can be a foundation for subsequent studies which would have for objectives to support the research on the influence of the variation of a number of parameters related to the functioning of the piston (material quality, design and geometric shapes, cooling parameters etc.).

Better safety factors can be aimed by the improvement of the design, the materials and by the strengthening of the cooling by oil.

REFERENCES

Arques, P. (1987). *Moteurs Alternatifs à Combustion Interne*. Paris, Masson.

Hedhli, T. and Mejri, S. (2007). A thermomecanic pattern of a piston of engine with an internal combustion cooling air. *CMSM'2007*, Monastir-Tunisie.

Jault, J. (2001). *Techniques de l'ingénieur M4611*. Caractéristiques mécaniques des alliages d'Aluminium.

Keita, O., Hedhli, T. and Bessrour, J. (2014). Model for dynamic behavior of the crankshaft of an air cooled Diesel engine subjected to severe functionning. *Int. J. Automotive Technology* **15**, **5**, 823−833.

Laurent, M. and Vuillermoz, P. L. (1993). *Techniques de l'ingénieur K420*. Conductivité Thermique des Solides.

Li, C. H. (1986). Thermoelastic behavior of an aluminium diesel engine piston. *SAE Paper No*. 860163.

Monro, R., Dubois, F. and Matteoda, P. (1990). Ferrous Diesel Pistons for Highway Application. T&N, Technology for the 90 s, Paper No. 17.

Reipert, P., Moebus, H. and Schellmann, K. (1984). Computer aids piston design for high load in medium speed engines. *Diesel & Gaz Turbine Worldwide*, Juillet – Aôut, 25−28.

Silva, F. S. (2006). Fatigue on engine pistons – A compendium of cases studies. *Engineering Failure Analysis* **13**, **3**, 480−492.

Szmytka, F., Salem, M., Rézaï-Aria, F. and Oudin, A. (2015). Thermal fatigue analysis of automotive diesel piston: Experimental procedure and numerical protocol. *Int. J. Fatigue*, **73**, 48−57.

Tahar Abbes, M., Hadj Miloud, M. and Maspeyot, P. (2001). Un modèle global de pistons de moteur à combustion interne, Partie III – Le modèle thermique. *XVème Congrès Français de Mécanique*, Nancy.

Techniques de l'ingénieur B2800 (1996). Technologie des Moteurs à Combustion Interne.

Techniques de l'ingénieur BM 2900 (2004). Analyse des Transferts énergétiques dans les Moteurs Automobiles.

Wang, Q., Yiding, C. and Gang, C. (1995). Piston assembly design for improved thermal-tribological performance. *50th Annual Meeting in Chicago*, Illinois, USA.